Calculation of Nuclear Quadrupole Parameters in Imidazole Derivatives and Extrapolation to Coenzyme B_{12}. A Theoretical Study

Maricel Torrent, Djamaladdin G. Musaev, and Keiji Morokuma*

Cherry L. Emerson Center for Scientific Computation and Department of Chemistry, Emory University, Atlanta, Georgia 30322

Shyue-Chu Ke and Kurt Warncke

Department of Physics, Emory University, Atlanta, Georgia 30322

Received: May 19, 1999

The ^{14}N nuclear quadrupole coupling (NQC) constants (χ) and asymmetry parameters (η) for a series of small nitrogen-containing imidazole derivatives are investigated, by using density functional theory (DFT), in three clearly distinct environments: as free molecules, in the solid state, and in solution. The spectroscopic characterization is also extended to coenzyme B_{12} and cob(II)alamin systems. The main findings can be summarized as follows: (i) Deviations in the calculated χ for the two nitrogen sites in the free imidazole molecule are small enough to allow quantitatively accurate predictions for isolated molecules of substituted benzimidazole compounds. (ii) Asymmetry parameters, however, are difficult to reproduce with accuracy; only *trends* along a series of compounds can be taken as informative. (iii) Shifts of the NQC parameters on going from gas phase to solid state are reasonably well reproduced at a qualitative level by using a trimer model; to reach similar levels of accuracy in the case of η, both the continuum and the point-charge effects need to be included. (iv) Short-range effects play an important role in the ^{14}N NQC parameters of imidazole in solution, although the NQC constants are also sensitive to solvent molecules beyond the first shell. (v) Long-range effects taken into account by an averaged continuum model alone are not enough to reproduce the effect of hydrogen bonding with water on the ^{14}N NQC parameters of imidazole; whenever water molecules are present, these solvent molecules have to be included explicitly. (vi) Metal−ligand interactions are relevant only for the NQC parameters of the proximal N, more specifically for the η value of this atom; most of the environmental effects in the real coenzymes are handled correctly by employing a solvated nonmetallic model. (viii) We estimate that the χ and η for the *proximal* nitrogen atom in cob(II)alamin (which so far has escaped experimental observation) will be approximately 2.7 MHz and 0.8, respectively, as indicated by our calculations.

I. Introduction

Imidazole is a fundamental component of many proteins, in particular as a constituent of the amino acid histidine.[1] Because the imidazole nitrogens are in the side-chain of protein, they form readily available bonding sites for metal ions.[2] Indeed imidazole nitrogens have been assigned an important role in the functioning of many metalloenzyme systems; their involvement is particularly noticeable in the binding of zinc in carboxypeptidase,[3] carbonic anhydrase,[4] yeast alcohol dehydrogenase,[5] and superoxide dismutase,[6] and last but not least, in the binding of cobalt in coenzyme B_{12}.[7]

Coenzyme B_{12} is a biologically important compound[8] characterized by a cobalt(III) center directly bound to five nitrogen ligands: four from the corrin ring (a heme system lacking one bridging CH group) in the equatorial plane and one from the α-axial dimethylbenzimidazole ligand. A sixth ligand, R, on the β-face above the macrocycle in the orientation in Figure 1, completes the octahedral coordination around the metal center. The structural changes that occur during the Co−R bond homolysis of the coenzyme, which is a transition from a cobalt(III) corrin (**1**) to a cobalt(II) corrin (**2**) (B_{12r}), are still unknown despite extensive experimental[9] and theoretical[10] work. As a first approach to elucidate the factors promoting such a cleavage, the understanding of the properties of these biologically important species is of great current interest.[11] The property we focus on here is the nuclear quadrupole coupling (NQC)[12] associated with the ^{14}N nuclei in the α-axial ligands of these molecules.

NQC parameters are a measure of the coupling between the ^{14}N nuclear quadrupole moment and the electric field gradient (EFG) at a given nucleus site due to the nonspherical charge distribution in the system.[13] Such interactions can be measured either in the gas phase (using microwave spectroscopy) or in solids (mostly by nuclear quadrupole resonance (NQR) spectroscopy). A fundamental difficulty in NQR with more than one ^{14}N nucleus in a similar environment (like in **1** or in **2**) is to determine which signals relate to which center, providing that they can be obtained for all centers.

A recent ESEEM (electron spin−echo envelope modulation) experiment on cob(II)alamin (**2**) has provided[14] unique information on one of the two ^{14}N nuclei in the 5,6-dimethylbenzimidazole axial ligand (the remote nitrogen). To the best of our knowledge, no NQC data has been reported yet for coenzyme B_{12} (**1**). As it has been shown in related studies,[15] the NQC parameters at the coordinated N atom are a sensitive indicator of binding to the metal center, so that rather detailed inferences regarding the extent of electron transfer can be obtained from the NQR data of this nucleus. However, ESEEM from the *proximal* dimethylbenzimidazole nitrogen in **2** (which is actually

10.1021/jp991612c CCC: $18.00
Published on Web 09/23/1999

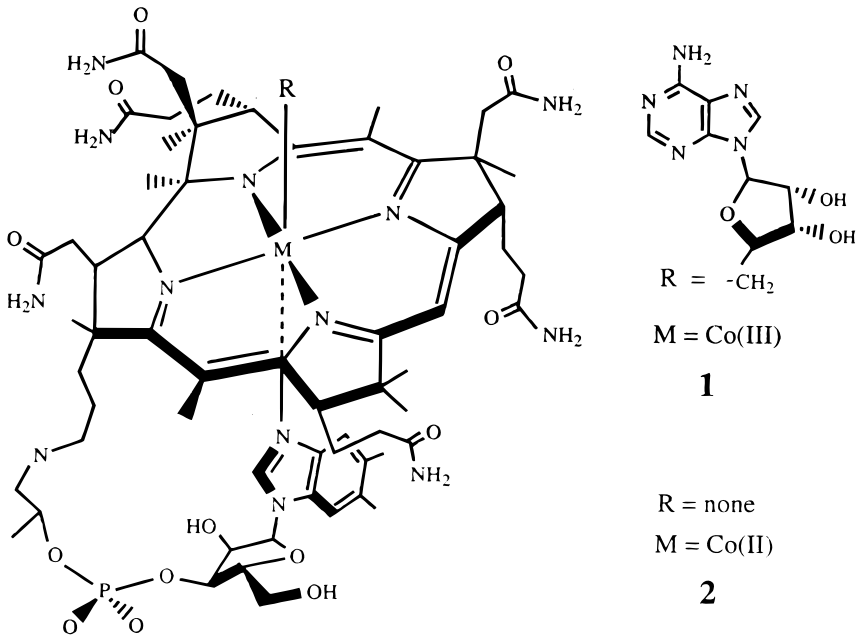

Figure 1. Molecular structure of coenzyme B_{12} (**1**) and cob(II)alamin B_{12r} (**2**).

bonded to Co) escaped observation because the couplings for this nitrogen are shifted beyond the ESEEM frequency window.[14] Having such a piece of information would be essential, and computation may be able to provide some estimate for the missing data.

The EFG at a nucleus in a molecular environment is a one-electron property that can be obtained with a reasonable effort from ab initio calculations. Since it involves only the ground state wave function, it should be much more readily calculated than for instance the chemical shift in nuclear magnetic resonance. However, there has been much less theoretical effort devoted to the interpretation of nuclear quadrupole resonance than to nuclear magnetic resonance.[16] The lack of theoretical activities in the NQC is likely to be due to the fact that most practical measurements of the NQC are made in the solid by the NQR spectroscopy, except for a few in gas phase using the microwave spectroscopy. The observed shifts in the nitrogen NQCs on going from the free monomer to the solid are often quite large for many nitrogen compounds. Therefore a direct comparison of the calculated NQC parameters for a free molecule cannot be made with the solid experiments. For instance, NQR studies for NH_3 and HCN have shown[17] that the ^{14}N EFGs are reduced from their free monomeric values by approximately 20% and 16%, respectively. In heterocyclic compounds, such as tetrazole and imidazole, even larger ^{14}N shifts (ranging from 30 to 40%) are observed. Such large shifts are considered to be due to the short-range hydrogen bonding interactions as well as the long-range electrostatic interactions in the solid. A few theoretical studies of NQC parameters in solid states have been published,[18] although they are not always very successful.[19]

Evaluation of NQC parameters in solution and in biomolecules and large metal complexes is a related area that has not been much explored yet from a computational point of view. Water is known to be a crucial component for both the structural integrity and functioning of biological systems such as coenzyme B_{12}. ^{14}N NQC should reflect the effect due to water-biomolecular interactions. To simulate the NQC in such condensed phase environments, one has to include the effect of interaction of the probe molecule with other molecules, water, and biological environments. In the present paper, we evaluate and compare ^{14}N NQCs for a series of imidazole derivatives (methyl-substituted imidazole and benzimidazole molecules) in three clearly distinct environments: as free molecules, in the solid state, and in solution. The largest member of the selected series (*N*-methyl-5,6-methylbenzimidazole) corresponds exactly to the actual α-axial ligand present in coenzyme B_{12} (**1**) and in cob(II)alamin (**2**). Therefore, the NQC parameters for both proximal and remote nitrogens in these systems can be extrapolated, as a first approximation, from the parameters in the "hydrated" *N*-methyl-5,6-methylbenzimidazole ligand. The paper is completed with a final section devoted to the simulation of metal−ligand interactions in the real biomolecular systems **1** and **2**.

In the next section we summarize the computational procedures, and test various ab initio and DFT methods and basis sets for a small nitrogen-containing benchmark molecule (NH_3).

II. Computational Methods and Calibration Calculations

The formulation employed in the evaluation of NQC parameters can be found elsewhere.[20] Briefly, the EFG is a traceless, symmetric second-rank tensor whose principal axes are chosen so that its components satisfy[21] $|q_{zz}| \geq |q_{yy}| \geq |q_{xx}|$ ($q_{ij} = \partial^2 V/\partial i \partial j$ where $i, j = x, y$, and z, and V is the external electrostatic potential). The quantities usually determined experimentally are the NQC constant, $\chi = e^2Qq/h$ (where Q is the nuclear electric quadrupole moment and $q = q_{zz}$), and the asymmetry parameter, $\eta = |(q_{yy} - q_{xx})/q_{zz}|$. As in many previous works,[22] here we assume that the nuclear quadrupole moment acts as a simple constant or scaling parameter, and we do not parametrize it (as done in some other works[23]). Among the wide range of $Q(^{14}N)$ standard values published,[24] we have selected the recent $Q(^{14}N)$ value of $20.44(3) \times 10^{-31}$ m^2 reported by Tokman et al.[25]

To select the most suitable method for computing the NQC parameters, we have performed some test calculations on ammonia, for which the NQC constant in gas phase is well established ($\chi_{exptl} = 4.09$ MHz).[26] The results are shown in Table 1. A variety of methods (including both ab initio and DFT) and basis sets have been employed. As can be seen from Table 1, the EFG is rather insensitive to the level of theory used, but it depends heavily on the size of the basis set. This is in good agreement with previous studies showing that large basis sets

TABLE 1: Nitrogen-14 NQC Constants of Ammonia[a] Using Different ab Initio and DFT Methods and Basis Sets[b]

method	basis set	q_{zz} (au)	χ (MHz)[c]	% error[d]	CPU time[e]
	I	1.097 923	5.27	28.8	1.00
HF	II	0.974 229	4.68	14.4	1.05
	III	0.947 895	4.55	11.2	1.10
	I	1.041 989	5.00	22.2	1.41
MP2	II	0.891 733	4.28	4.6	1.71
	III	0.849 123	4.08	−0.2	2.64
	I	1.063 413	5.11	24.9	2.42
MP3	II	0.927 423	4.45	8.8	3.71
	III	0.884 061	4.25	3.9	12.63
	I	1.062 986	5.10	24.7	2.68
MP4SDQ	II	0.925 408	4.44	8.6	4.29
	III	0.884 215	4.25	3.9	13.61
	I	1.066 907	5.12	25.2	3.42
CISD	II	0.934 106	4.49	9.8	4.70
	III	0.895 315	4.30	5.1	14.98
	I	1.062 094	5.10	24.7	3.65
QCISD	II	0.926 074	4.45	8.8	7.01
	III	0.885 657	4.25	3.9	12.75
	I	1.062 744	5.10	24.7	3.09
CCD	II	0.925 690	4.45	8.8	5.78
	III	0.883 433	4.24	3.7	16.63
	I	1.092 452	5.25	28.4	1.93
B3LYP	II	0.932 285	4.48	9.5	3.79
	III	0.905 317	4.35	6.4	5.53
	I	1.094 061	5.25	28.4	2.56
BLYP	II	0.914 897	4.39	7.3	3.92
	III	0.888 489	4.27	4.4	4.91
	I	1.055 062	5.07	24.0	2.26
BPW91	II	0.906 045	4.35	6.4	3.27
	III	0.880 745	4.23	3.4	4.47
	I	1.097 661	5.27	28.8	1.59
PW91LYP	II	0.903 819	4.34	6.1	2.98
	III	0.877 004	4.21	2.9	3.82
	I	1.053 582	5.06	23.7	1.57
PW91P86	II	0.884 998	4.25	3.9	3.52
	III	0.859 478	4.13	1.0	4.38

[a] At geometries optimized at the B3LYP/6-31G(d,p) level. [b] Basis set notation: I = 6-311G**, II = 6-311++G**, III = 6-311++G(2d,2p). [c] Using Q(^{14}N) from ref 25 to transform the EFG to the χ tensor. [d] Evaluated as $(\chi_{calc} - \chi_{exptl})/\chi_{exptl}$. [e] Relative to the HF/I calculation.

are often necessary to obtain reliable EFG values.[27] All calculated NQC values in Table 1 overestimate the experimental value systematically, the only exception being with one of the MPn methods ($n = 2$, basis set III) where the computed value is below the experimental reference by only 0.1 MHz. Such a coincidence between experiment and theory has been regarded as suspiciously fortuitous, probably because of an artifact of the MP2 method (an additional indication is that there is no improvement upon going to $n = 3$, 4, where the error has the same sign as in the rest of the table), and therefore, MP2 has been discarded as a reliable method to be employed in this study. Among the levels of calculation examined in Table 1, we have selected the PW91P86/III as the one best fitting the criteria: performance and computational cost. This will be the method and basis set used throughout the paper.

Table 2 gathers five different test calculations for the parent imidazole. The first is our standard method, PW91P86/III//B3LYP/I, selected from the results in Table 1. Additional calculations have been done here to test whether the use of the experimental geometry[28] (entry 2) or a larger basis set for geometry optimization (entries 3−5) would significantly affect the calculated NQC parameters. Also in entries 4 and 5, the question whether the use of the same basis set for geometry optimization and evaluation of the property would help improve the results has been addressed. All these additional tests have been prompted by previous studies[29] showing that the EFG is very sensitive to geometry changes and that the best results were often obtained using the experimental geometry. In a more recent theoretical study on the nitroethene molecule,[30] however, minor differences were found between the values obtained at the experimental and optimized geometries. As can be seen from Table 2, there is neither systematic nor significant improvement when any of such modifications on the molecular geometry is applied in our particular case. The best result for the NQC constant χ, in the parent imidazole comes from the standard method, with deviations of only 4.0% and 1.1% for NH and N, respectively.[21]

TABLE 2: Calculated (and Experimental in Italics) Nitrogen-14 NQC Constants χ (in MHz) and Asymmetry Parameters η for the Parent Imidazole in the Gas Phase Using Different Methods

method	NX (tricoordinate		N (bicoordinate)	
	χ	η	χ	η
PW91P86/III//B3LYP/I	2.639	0.133	4.076	0.067
PW91P86/III//exptl geometry[a]	2.558	0.091	4.089	0.050
B3LYP/III//PW91P86/III	2.618	0.129	4.128	0.073
B3LYP/III//B3LYP/III	2.750	0.121	4.401	0.105
PW91P86/III//PW91P86/III	2.659	0.135	4.077	0.053
exptl[b]	2.537	0.1778	4.032	0.1200

[a] Reference 28. [b] From microwave data reported by Blackman et al. (ref 35).

Full (unless otherwise indicated) optimization of geometries has been carried out at the B3LYP/I level for the nonmetallic systems, and at the B3LYP/LANL2DZ level for the cobalt-containing models. The evaluation of the one-electron property has been done at the PW91P86/III//B3LYP/I and PW91P86/LANL2DZ//B3LYP/LANL2DZ levels for nonmetallic and metallic systems, respectively. Simulation of the effects from the lattice in solid state has been performed by adding a background charge distribution[31] to the trimer of imidazole. In particular, a set of electrostatic potential-derived charges generated by the Merz−Singh−Kollman scheme[32] has been placed at the nearest neighboring atoms in the real crystal. Both short-term and long-term effects of solvation on EFGs have been also considered. Short-term solvation effects have been investigated with a supermolecule approach only for the parent imidazole molecule. Long-term solvation effects have been analyzed for the entire set of molecules by means of reaction field calculations using the polarizable dielectric model of Tomasi and coworkers.[33] All calculations have been carried out with the Gaussian 98 package.[34]

III. Results and Discussion

First, we present the NQC constants and asymmetry parameters computed for a series of five imidazole derivatives: the parent imidazole, *N*-methylimidazole, benzimidazole, *N*-methylbenzimidazole, and *N*-methyl-5,6-dimethylbenzimidazole, as free molecules, and we compare them with the microwave data (available only for the smaller member of the series).[35] The B3LYP/I optimized geometries for this series of compounds are shown in Figure 2. Second, we perform calculations for the trimer of imidazole as a model of solid imidazole, and we include the effect of the surroundings on the NQC parameters. Third, we simulate the role of solvation by water molecules in the whole series of imidazole derivatives, and compute the corresponding NQCs in solution. Finally, we also evaluate the influence of the metal−ligand interactions on the studied property by using small cobalt-containing models for **1** and **2**.

A. Free Molecules. Table 3 shows the computed NQC parameters for the target molecules in Figure 2. Before we start

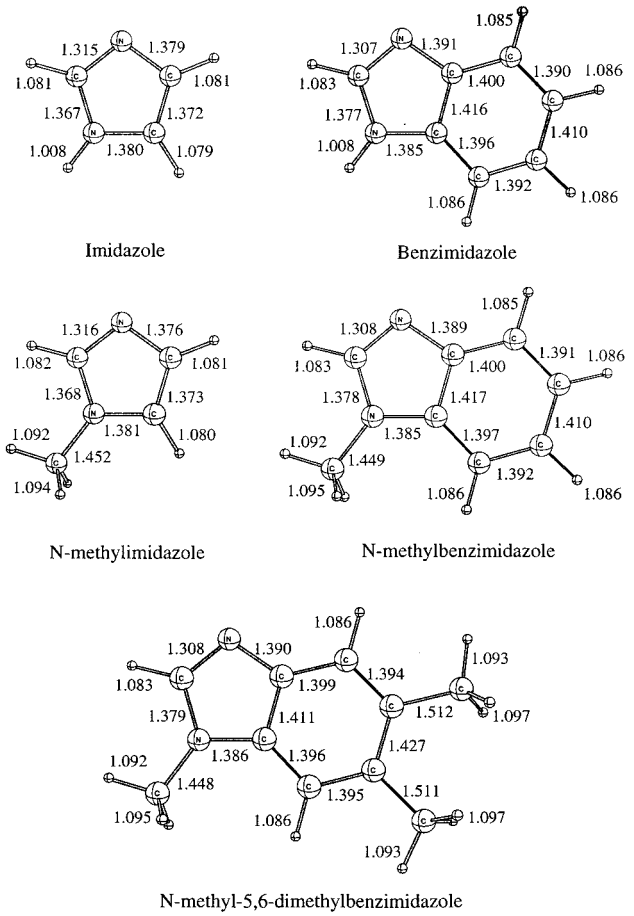

Figure 2. Optimized molecular structure (bond distances in angstroms) of imidazole and its derivatives at the B3LYP/I level.

TABLE 3: Calculated and Experimental Nitrogen-14 NQC Constants χ (in MHz) and Asymmetry Parameters η for Imidazole and Its Derivatives in the Gas Phase at the PW91P86/III Level Using the B3LYP/I Optimized Geometries

	NX (tricoordinate)		N (bicoordinate)	
compound	χ	η	χ	η
imidazole	2.639	0.133	4.076	0.067
exptl[a]	(2.537)	(0.1778)	(4.032)	(0.1200)
N-methylimidazole	2.785	0.351	4.016	0.045
benzimidazole	3.275	0.073	3.863	0.041
N-methylbenzimidazole	3.397	0.229	3.775	0.071
N-methyl-5,6-dimethylbenzimidazole	3.442	0.230	3.763	0.083

[a] Reference 35.

discussing compound by compound, it is worth noting that the χ values for the pyrrole-like nitrogen (column 2) are smaller than for the pyridine-like nitrogen (column 4) regardless of the compound. As the lone-pair orbitals contribute most to the χ value of ^{14}N in nitrogen-containing heterocyclic molecules, it is expected that the lone-pair character will be more pronounced in the bicoordinate nitrogen than in the tricoordinate nitrogen, where the lone-pair electrons is conjugated with the π-system of the ring, thus giving smaller χ values.

As discussed in the preceding section, the computed NQC constant χ in the parent imidazole (using the standard method) deviates only 4.0% for NH and 1.1% for N.[21] Larger deviations, however, are observed in the case of the asymmetry parameter η, as was found previously for other systems.[36] This discrepancy has been found even in the comparison of values derived from complex CI calculations and from gas-phase microwave data.[27,37] In η, the three diagonal components of the EFG are involved in its definition. Each of them is a very small difference between two large numbers, the electronic and the nuclear contribution. Therefore, a change of only a few percent in any of these large numbers has dramatic effects on η. This problem is particularly severe when q_{yy} and q_{xx} are very close, because a minute fractional shift in one of them automatically generates a large variation in η. As seen from the definition of η, variations in q_{zz} also contribute to its change but in a lesser degree than the two other components. Consequently, unless each of the q_{ii}'s is computed to an extremely high accuracy, η will possess much larger uncertainties than χ which only contains q_{zz}. This requirement has been suggested to be the main reason in most papers dealing with EFG calculations only χ is reported.[38]

Since there is no experimental results for *N*-methyl imidazole, benzimidazole, and its derivatives in gas phase, the calculated values in Table 3 constitute theoretical predictions. The degree of substitution in the parent imidazole has different effects on the coupling constants χ of the tricoordinate and bicoordinate nitrogen atoms. The computed χ values increases for tricoordinate N atoms in the order: imidazole → *N*-methylimidazole → benzimidazole → *N*-methylbenzimidazole → *N*-methyl-5,6-methylbenzimidazole, while it decreases in the same order for bicoordinate N atoms. Thus, heavily substituted imidazoles tend to have nearly equal χ values for the tricoordinate and bicoordinate nitrogen atoms.

When H is replaced by a methyl group at the tricoordinate N site, η on this atom increases noticeably, as seen in Table 3: about 2.6 times from imidazole to *N*-methylimidazole, and more than 3 times in the benzimidazole/*N*-methylbenzimidazole pair. A similar trend has been reported by Huber et al.[39] in a recent study on pyrrole and *N*-methylpyrrole. In a previous theoretical study, the η value for *N*-methylpyrrole (0.300) was found to be much larger than that for pyrrole (0.112), although the EFGs along the molecular symmetry axes calculated at the N sites were found not to differ much (q_{zz} = 0.6034 au for pyrrole, and 0.5992 au for *N*-methylpyrrole).[39] For hydrazine and methylhydrazine,[40] it was also shown that the χ and η values were significantly influenced by methyl substitution on the nitrogen atom. Comparison of our results for the last two rows in Table 3 indicates that none of the two nitrogen atoms in the imidazole ring becomes much affected by the substitution of methyl groups in the distant γ-C atoms.

B. Simulation of the Solid State. *Imidazole Trimer Model.* Several studies have utilized NQR spectroscopy to obtain the NQC parameters for imidazole in the solid state.[41,42] Unlike in the gas phase, in the solid the entire lattice contributes to the EFG at the ^{14}N nuclei so that the NQC parameters are quite different from those of an isolated imidazole molecule. Also, X-ray diffraction studies[43] have shown H-bonding to be strong enough in the solid to make the two nitrogen atoms almost structurally equivalent. This leads to a substantial change in the electronic structure at the N atoms, and therefore, a suitable model must be employed to reproduce such a change.

The crystal structure of imidazole at 103 K by neutron diffraction[44] revealed that imidazole is monoclinic, crystallizes in space group $P2_1/c$, with $Z = 4$ molecules per unit cell, and has lattice parameters a = 7.569(1), b = 5.366(1), c = 9.785(2) Å, and β = 119.08(1)°. A unit cell with $Z = 4$, however, makes it impracticable to compute one group of four molecules with a full shell of neighbors. Our model, in Figure 3, has been selected taking into account that in the crystal each of the two distinct nitrogen sites per imidazole molecule participates only in *one* hydrogen bonding interaction. Therefore, three molecules

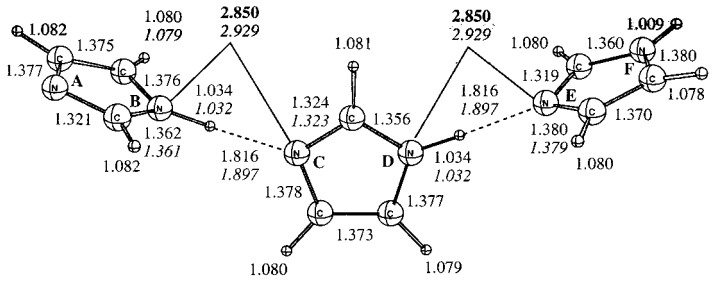

Figure 3. Partially (in bold when fixed) and fully (shown only when different, in italic) optimized structure (bond distances in angstroms) of the trimer of imidazole at the B3LYP/I level.

TABLE 4: Calculated Nitrogen-14 NQC Constants χ (in MHz) and Asymmetry Parameters η for the Trimer of Imidazole at the PW91P86/III Level, at the Partially and Fully Optimized Structures

	partially optimized		fully optimized	
molecular site	χ	η	χ	η
NH (tricoordinate)				
N_B	1.678	0.754	1.795	0.588
N_D	1.631	0.798	1.744	0.633
N_F	2.504	0.074	2.514	0.079
(exptl NQR in solid)[a]	(1.418)	(0.997)		
(exptl MW in gas phase)[b]	(2.537)	(0.1778)		
N (bicoordinate)				
N_A	3.999	0.039	4.004	0.040
N_C	3.542	0.086	3.566	0.073
N_E	3.560	0.070	3.583	0.058
(exptl NQR in solid)[a]	(3.253)	(0.135)		
(exptl MW in gas phase)[b]	(4.032)	(0.1200)		

[a] Reference 41. [b] Reference 35.

are expected to be enough to reproduce the first shell interactions. A support to the choice of our model is provided by a previous theoretical study[45] where the solid state of tetrazole (which has *four* distinct nitrogen sites per molecule) was simulated at the dimer level. In that study, it was demonstrated that the H-bond interactions were largely complete with only two molecules, and the authors concluded that restricting calculation to a dimer should not be a serious limitation.[45] In a more recent study on solid quinoxalinones, it was also shown[46] that a trimer of molecules was enough to simulate the environment of one molecule in the solid.

The structure of the imidazole trimer, fully optimized and partially optimized, with the intramolecular distance N···N involved in hydrogen bonding kept frozen to the value observed in the solid (2.850 Å),[44] are shown in Figure 3. The fully optimized structure shows the weakening of the hydrogen bonding interactions with shorter N−H distance and longer H···N distance, as compared to that of the crystal experiment.

The calculated ^{14}N NQC parameters for partially and fully optimized structure of the imidazole trimer are shown in Table 4. In the trimer model, as seen in Figure 3, N_C and N_D should represent the nitrogen atoms in the crystal, while other nitrogens are to represent those on imidazole with a single hydrogen bond. The results in Table 4 are consistent to this expectation. The NQC parameters of N_E and N_B, the nitrogens involved directly in the hydrogen bonding but on a single-H-bonded imidazole, are only slightly different from those of N_C and N_D, suggesting the effect of H-bond on the other nitrogen in the same imidazole molecule is not very large. The NQC parameters for the fully optimized structure is slightly less like those in solid than for the partially optimized structure, as expected from the geometry differences discussed above.

The calculated NQC constant and asymmetry parameter for the H-donor tricoordinate N_D site in the simulated solid imidazole, 1.63 (MHz) and 0.78, are significantly reduced and increased, respectively, from the gas-phase values, 2.64 and 0.13. On the other hand, those for the H-acceptor bicoordinate N_C site, 3.54 (MHz) and 0.09, are remarkably reduced and slightly decreased, respectively, from the gas phase values, 4.08 and 0.07. These changes reproduce the trends of the experimental changes very well. However, compared to the solid state experiments, the changes are not large enough; obviously the long-range effect of the solid is missing from the calculation.

Assuming that the ratio between the experimental or computed NQC parameters for solid imidazole (Table 4) and the corresponding values for gas-phase imidazole (Table 3) is independent of the molecule, estimates of the solid values for other molecules can be calculated. The calculated (and experimental, in parentheses) changes in the imidazole nitrogen NQC parameters on going from the free monomer (Table 3) to the solid (for computed values using N_C and N_D from Table 4) are for the bicoordinate N, a decrease by 14 (19)% in χ and an increase by 36 (13)% in η, and for the tricoordinate N, a decrease by 38 (44)% in χ and an increase by 5.8 (5.6) times in η. If one uses these ratios and the calculated gas-phase values (Table 3), one obtains estimates of the solid molecule: $\chi = 3.32$ (3.13) MHz and $\eta = 0.056$ (0.046) for the bicoordinate N, and $\chi = 2.03$ (1.83) MHz and $\eta = 0.42$ (0.41) for the tricoordinate N. These may be compared with the experimental NQC parameters in the solid:[41] $\chi = 3.140$ MHz and $\eta = 0.303$ for the bicoordinate N; $\chi = 1.960$ MHz and $\eta = 0.786$ for the tricoordinate N. Comparison of these values indicates that, regardless whether one uses the calculated or experimental ratios, extrapolations from gas to solid give good estimates for χ within 6−7% of experiment, but only qualitative estimates at best for η.

One should note that the value of η for the tricoordinate N site is the largest asymmetry parameter yet observed in a nitrogen compound (0.997).[42] This implies an unusual situation that the electric field environment is nearly in D_{3h} symmetry with $q_{yy} \approx q_{zz}$ (in plane) and $q_{xx} \approx 0$ (out of plane). The trimer models cannot reproduce this situation.

Inclusion of the Continuum and the Point-Charge Effects. To obtain more quantitatively significant results for η, the effect of the lattice has been simulated by means of two different approaches, as shown in Table 5: (1) by using a continuum model (PCM) of Tomasi et al.[33] and (2) by locating selected point charges around the trimer of imidazole which reproduce the permanent electrostatic potential from the neighbors.

For approach (1) we should use the solid dielectric constant for imidazole. Without such data, we adopted $\epsilon = 4.5$ (for solid imidazole) and 9.0 (for liquid imidazole) from the experimental dielectric constants for other related small amines [(in solid) ethylenediamine, 5.9; (in liquid) ethylenediamine, 12.9; pyrrole, 8.00; pyrrolidine, 8.30; pyridine, 13.26; aniline, 7.06; quinoline, 9.16; isoquinoline, 11.0; nicotine, 8.937)][47] and the fact that

TABLE 5: Calculated Nitrogen-14 NQC Constants χ (in MHz) and Asymmetry Parameters η for the Trimer of Imidazole at the PW91P86/III Level, at the Partially Optimized Structure, Surrounded by Either a Polarized Continuum Model (PCM, $\epsilon = 9.00$ for Liquid, and $\epsilon = 4.50$ for Solid) or Point-Derived Charges

	PCM ($\epsilon = 9.00$)		PCM ($\epsilon = 4.50$)		point-derived charges	
molecular site	χ	η	χ	η	χ	η
NH (tricoordinate)						
N_B	1.548	0.879	1.567	0.859	1.641	0.809
N_D	1.468	0.993	1.488	0.966	1.685	0.831
N_F	2.137	0.186	2.208	0.135	2.508	0.084
(exptl NQR in solid)[a]	(1.418)	(0.997)				
(exptl MW in gas phase)[b]	(2.537)	(0.1778)				
N (bicoordinate)						
N_A	3.843	0.013	3.870	0.017	4.019	0.043
N_C	3.361	0.138	3.384	0.131	3.457	0.158
N_E	3.344	0.120	3.381	0.111	3.560	0.067
(exptl NQR in solid)[a]	(3.253)	(0.135)				
(exptl MW in gas phase)[b]	(4.032)	(0.1200)				

[a] Reference 41. [b] Reference 35.

the solid values are usually much smaller than the liquid values. As can be seen from Table 5, inclusion of the continuum improves the computed parameters dramatically (compare with Table 4), especially the asymmetry parameters, and more specifically the unusual $\eta = 0.997$ observed for the tricoordinate N. It follows that the polarity in the real system does play an important role, and that the continuum model herein employed accounts for the difference between the isolated trimer (Table 4) and the trimer affected by neighboring interactions (Table 5).

For the second approach we calculated the Merz−Singh−Kollman[32] point charge on each atom in the imidazole molecule, and placed them, as a simple model, only in the site of the four nearest imidazole molecules neighboring the central ring in the trimer: one above, one below, one behind, and one in front (see Figure 4). The corresponding χ and η values are shown in Table 5. Again the calculated parameters resemble very much the ones from experiment, although to a lesser extent than by using a PCM model. This is due to the implicit limitations of simulating with point charges only *four* of the molecules surrounding the central imidazole. The use of a larger number of point charges, e.g., including several shells, should shorten the difference between experiment and theory. However, the model in Figure 4 is good enough to reproduce the right trend. Also, it should be noted that, since the selected point charges have been located around the *central* imidazole molecule, the terminal N atoms (N_A and N_F) present values much closer to gas-phase than N_A and N_F in the PCM model, where the whole trimer is surrounded by a polarized continuum.

C. Simulation of the Solvent Environmental Effects in the Coenzyme. Water is known to be an important component in biological systems such as coenzyme B_{12}.[48] Protein crystals often contain between 40 and 60% solvent, and the effects of water−water and water-biomolecular interactions have to be considered. Unfortunately, usually relatively little is known about the exact positions and orientations of the hydration layers around biomolecules. Coenzyme B_{12} is not an exception. Given the uncertainty of the resolved water-structures,[49] we have decided to investigate both short- and long-range effects of water surroundings on the NQC parameters.

Cluster with Four Water Molecules. Calculations simulating short-range solvent effects have been carried out for the imidazole molecule, with four water molecules (two per each N site) initially located around it. After fully optimizing the geometry, only one water molecule per N site kept its interaction with the nitrogen, and the other two molecules migrated to the second solvation sphere, as shown in Figure 5. The computed NQC parameters for this solvated imidazole are shown in the first row of Table 6. It is interesting to note that the computed value of η for the tricoordinate N (0.568) is midway between the one for the free imidazole molecule (0.133 in Table 3) and the one for the model solid imidazole (0.774, N_D in Table 4). On the contrary, the difference in η for the bicoordinate N is small among gas phase, solid, and water hydrogen-bonded environments.

Clusters with One and Two Water Molecules. In the previous paragraph, the importance of short-range effects has been shown. Now, it would be interesting to quantify how much a explicit solvent molecule attached to either the proximal or remote N atom affects the electronic environment of the *other* N atom (remote and proximal, respectively). For this purpose, we have evaluated the NQC constants for three different clusters, as shown in Figure 6. The computed values are gathered in rows 2−4 of Table 6. Inspection of these values leads us to conclude that addition of a solvent molecule to one of the N sites has little effect on the χ and η values of the other N. This is consistent with the fact mentioned in section B concerning the effect of H-bond on the other N in the same imidazole molecule. However, it is worth noting that the NQC constants are sensitive to solvent molecules beyond the first shell. Thus, on going from 2 H_2O (= only first shell; Figure 6) to 4H_2O (= first and second shell; Figure 5), the deviation from experimental values is notably reduced (Table 6).

Polarizable Continuum Model, without and with Explicit Water Molecules. An alternative approach for reproducing the electronic environment in solution is to take into account the long-range effects created by the distant water coat, using a polarized continuum model of Tomasi et al.[33] We performed such calculations, using the optimized geometries of free molecules for imidazole and benzimidazole derivatives, by surrounding each molecule by a continuum of $\epsilon = 78.39$, as shown also in Table 6. We also surrounded the imidazole + 4H_2O cluster by a continuum of the same ϵ to include both the short-range direct interaction and the long-range effects.

Comparison of the explicit water, PCM, and explicit water + PCM models for imidazole in Table 6 shows that long-range effects taken into account by the PCM model alone are not enough to reproduce the effect of hydrogen-bonding with water on the ^{14}N NQC parameters of imidazole. This is more important for η, especially for tricoordinate N. The direct hydrogen-bond effect on the NQC parameters is very local and very directed, and the averaged continuum model, even in its best PCM implementation, cannot mimic this environment. Therefore, in the situation where the direct interaction with water molecules exists, these water molecules have to be included explicitly. In the case of coenzyme B_{12}, no explicit water molecules have been reported to be present in the immediate surroundings of the dimethylbenzimidazole α-axial ligand. This is the reason we have considered only long-range effects of aqueous environment for imidazole derivatives in Table 5 (rows 7−10).

The NQC parameters for *N*-methyl-5,6-dimethylbenzimidazole (the species analogous to the actual ligand bonded to Co in the coenzyme) are indeed the most interesting from the predictive viewpoint of the current study. Our calculation gives the NQC parameters $\chi = 3.073$ MHz and $\eta = 0.111$ for the tricoordinate nitrogen in *N*-methyl-5,6-dimethylbenzimidazole, which are in good agreement with the experimental values reported for the remote nitrogen from ESEEM simulations in

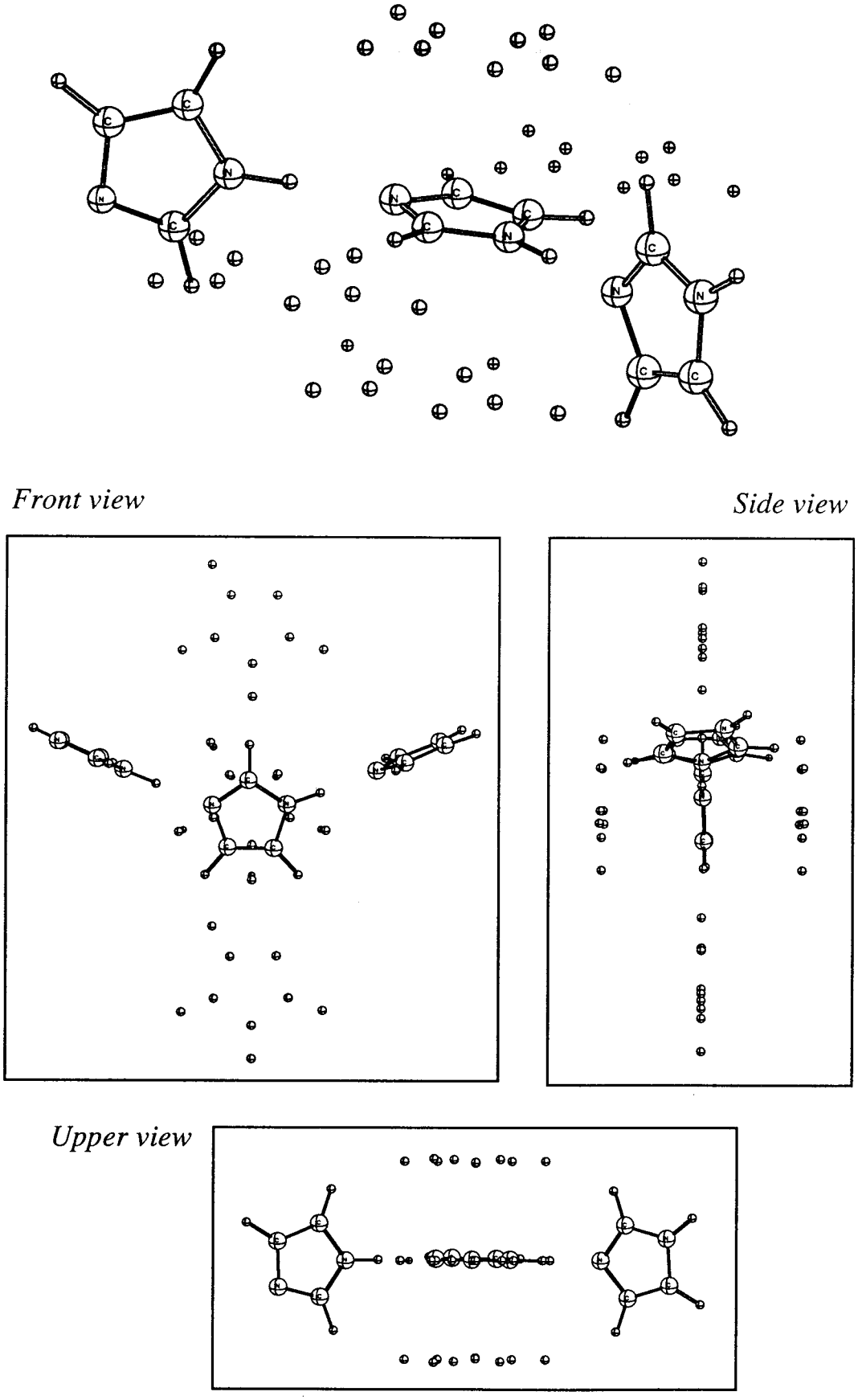

Figure 4. Different views of the trimer of imidazole surrounded by point charges at the location of the four nearest molecules in the crystal.

cob(II)alamin (**2**): $\chi = 3.2$ MHz and $\eta = 0.1$. As mentioned in the Introduction, ESEEM simulations for cob(II)alamin have not been able to estimate the NQC parameters for the proximal (bicoordinate) N. Using the small models in Figure 2 (purely organic, no metal present) our predictions for the bicoordinate nitrogen in *N*-methyl-5,6-dimethylbenzimidazole (Table 5) are

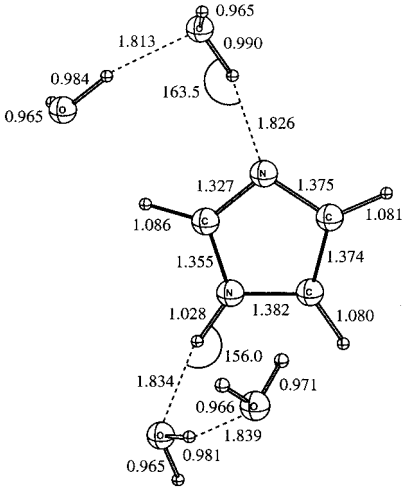

Figure 5. Optimized structure (in angstroms and degrees) of solvated imidazole at the B3LYP/I level.

$\chi = 3.402$ and $\eta = 0.231$, which we expect to be similar to those for the proximal N in cob(II)alamin.

D. Simulation of the Metal−Ligand Interactions in the Real Coenzyme. Up to this point we have used different approaches to take into consideration *most of the environmental effects* present in the axial ligand of the biomolecular systems **1** and **2**. A final question remains, however, concerning the effect that the Co atom might have on its immediate neighborhood and in particular on the proximal N atom. Metal−ligand interactions are unlikely to be well reproduced by considering only weak interactions (PCM) as in the previous sections. Although the absence of metal atoms in the models employed so far may not affect the NQC parameters of the remote N, it must have somehow a distinct effect on the bicoordinate N atom. Here we address this question by evaluating the one-electron property in two small cobalt-containing models (**3** and **4**, Figure 7) for coenzyme B_{12} (**1**) and B_{12r} (**2**), respectively. In previous theoretical studies on coenzyme B_{12}, a variety of models have been used, ranging from oversimplified to more sophisticated structures.[10] Unlike there, the purpose here is to compute the NQCs for the two nitrogens in the axial ligand. For this purpose, only the axial interactions deserve special attention. As seen from Figure 7, our model for the equatorial part (corrin ring) has been reduced to the essential components so that the computational cost keeps within reach. The results are summarized in Table 7.

The first entry of Table 7 displays the NQC parameters corresponding to the model of coenzyme B_{12} (**1**) for which experimental data has not been reported yet. Here our results serve as predictions to be confirmed by future experiments. The η value for the N directly attached to cobalt (i.e., the "bicoordinate" or better called "proximal" N in the metallic model) experiences a remarkable increase as compared to η for the same N in the gas-phase nonmetallic model (0.083, Table 3), and the NQC constant ($\chi = 2.441$ MHz) becomes 1.5 times smaller. The extent of these changes should be expected to be reduced in solution. On the other hand, the changes observed in χ and η for the *remote* (or tricoordinate) N on going from the nonmetallic to the metallic system are remarkably less significant. This is consistent with a much larger distortion of electron distribution around $N_{proximal}$ than around N_{remote} because of the presence of the metal atom.

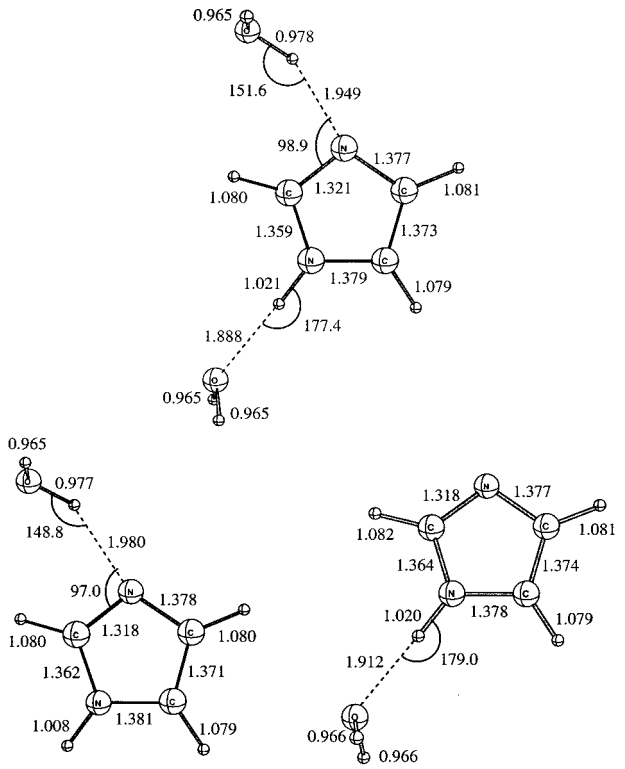

Figure 6. Optimized clusters (in angstroms and degrees) of one molecule of imidazole and one or two water molecules pointing toward the N sites.

The last two entries of Table 7 give the computed NQC parameters for cob(II)alamin (**2**) for which experimental data exists only for the remote N. If no polarized continuum model is added to model **4** (entry 2), our calculations for the proximal N yield an η value as high as 0.977, which would be again indicative of a strong distortion of the electron distribution around this N atom caused by the interaction with the central metal. Inclusion of a polarized continuum model (entry 4) reduces slightly the extent of this asymmetry, but still

TABLE 6: Calculated Nitrogen-14 NQC Constants χ (in MHz) and Asymmetry Parameters η for the Imidazole and Derivatives in Explicit Water and PCM Models of Aqueous Solution

		NX (tricoordinate)		N (bicoordinate)	
compound	model	χ	η	χ	η
imidazole	*4H2O*	1.816	0.568	3.494	0.091
	2H2O	2.061	0.311	3.664	0.024
	1H2O in N	2.577	0.115	3.708	0.014
	1H2O in NX	2.140	0.250	4.051	0.056
	4H2O + PCM	1.708	0.605	3.284	0.118
	Gas/PCM	2.639/2.097	0.133/0.229	4.076/3.591	0.067/0.039
benzimidazole	Gas/PCM	3.275/2.957	0.073/0.136	3.863/3.605	0.041/0.131
N-methylimidazole	Gas/PCM	2.785/2.420	0.351/0.211	4.016/3.607	0.045/0.047
N-methylbenzimidazole	Gas/PCM	3.397/2.992	0.229/0.098	3.775/3.459	0.071/0.201
N-methyl-5,6-dimethylbenzimidazole	Gas/PCM	3.442/3.073	0.230/0.111	3.763/3.402	0.083/0.231

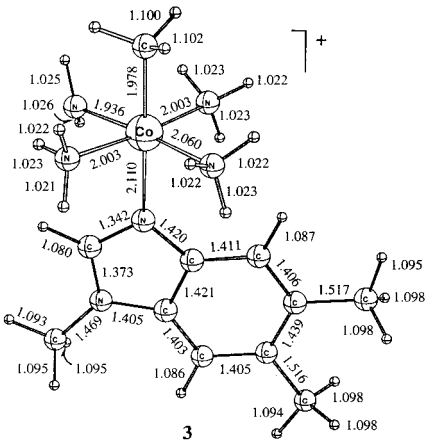

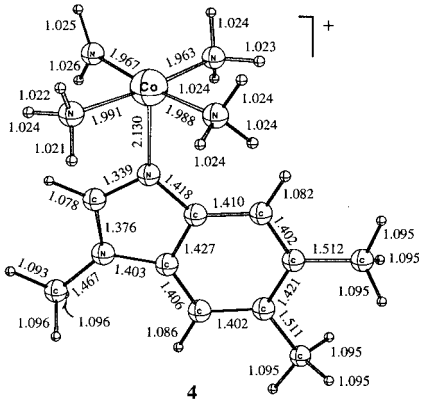

Figure 7. Optimized molecular structures (in angstroms) for simplified models of (top) coenzyme B_{12} and (bottom) B_{12r}.

TABLE 7: Calculated Nitrogen-14 NQC Constants χ_(in MHz) and Asymmetry Parameters η for Model Coenzyme 3 (without PCM), and for Model Coenzyme 4 (without and with a PCM)

	NX (remote)		N (proximal)	
model coenzyme	χ	η	χ	η
3	3.702	0.025	2.441	0.998
4	3.682	0.042	2.507	0.977
4 + PCM	3.639	0.049	2.724	0.842

points out to a significantly larger η than for the remote N, which does not seem to be much affected by the presence of the metal.

In conclusion, for the (so far uncharacterized) proximal N in cob(II)alamin (**2**) we expect a value of χ approximately to be 2.7 MHz and the η value around 0.8.

IV. Conclusions

According to the above presented results and discussions, we may draw the following conclusions:

(1) For small nitrogen-containing heterocycles such as the imidazole derivatives here studied, ^{14}N NQCCs in the gas phase can be confidently evaluated (and compared with microwave data) by using a density functional theory-based method and a basis set of medium quality.

(2) Deviations in the calculated NQCCs for the free parent imidazole molecule are small enough to allow *quantitative predictions* for isolated molecules of substituted benzimidazole compounds, whose NQC parameters are not available from experiment.

(3) Asymmetry parameters, however, are difficult to reproduce with accuracy. Calculated values are much affected by small changes in any of the involved components of the EFG tensor, and therefore, only *trends* along a series of related compounds should be taken as informative.

(4) Shifts of the NQC parameters on going from gas phase to solid state can be reasonably well reproduced at a qualitative level by using a trimer model. But here again, to obtain reliable values for the case of η, the model has to be improved, in particular, by including both the continuum and the point-charge effects.

(5) Short-range effects play an important role in the ^{14}N NQC parameters of imidazole in solution. It is found that the direct hydrogen-bond effect on the NQC parameters is very local and very directed.

(6) Despite it, the NQC constants are sensitive to solvent molecules beyond the first shell. On going from the model representing only first shell ($2H_2O$) to the model accounting for both first and second shell ($4H_2O$), the deviation from experimental values is significantly reduced.

(7) Long-range effects taken into account by an averaged continuum model alone are not enough to reproduce the effect of hydrogen-bonding with water on the ^{14}N NQC parameters of imidazole. In the situation where the direct interaction with water molecules exists, these water molecules have to be included explicitly.

(8) Metal−ligand interactions are only relevant for the proximal N, and, more specifically for the η value of this nitrogen atom. Most of the environmental effects in the real coenzymes can be handled well enough by employing a solvated nonmetallic model, provided that both short- and long-range interactions are simulated appropriately.

(9) The ^{14}N NQC parameters for coenzyme B_{12} have been reported here for the first time; we have also estimated that the χ and η for the *proximal* nitrogen atom in cob(II)alamin (which so far has escaped experimental observation) will be approximately 2.7 MHz and 0.8, respectively, as indicated by our calculations.

Acknowledgment. The use of the computational facilities and programs at the Emerson Center (Emory University) is acknowledged. The present research is in part supported by a grant (Grant CHE96-27775) from the National Science Foundation. Authors express their gratitude to Prof. Juha Vaara at the University of Oulu (Finland) for useful discussions. M.T. also acknowledges a Postdoctoral Fellowship from the Ministerio de Educación y Cultura of Spain.

Supporting Information Available: Full EFG tensor information obtained from computation for (1) imidazole as free molecule (gas-phase), (2) imidazole trimer model at the partially optimized structure, (3) imidazole: cluster with four water molecules, and (4) imidazole: cluster with two water molecules. This material is available free of charge via the Internet at http://pubs.acs.org.

References and Notes

(1) Ochiai, E.-I. *Bioinorganic Chemistry: An Introduction*; Busch, D. H., Shull, H., Eds.; Allyn and Bacon: Boston, 1977.

(2) (a) Wang, J. H. *Science* **1968**, *161*, 328. (b) Blow, D. M.; Birktoft, J. J.; Hartley, B. S. *Nature (London)* **1969**, *221*, 337. (c) Robillard, G.; Shulman, R. G. *J. Mol. Biol*. **1972**, *71*, 507. (d) Blow, D. M. *Acc. Chem. Res.* **1976**, *9*, 145.

(3) (a) Hartsuck, J. A.; Lipscomb, W. N. *The Enzymes*; Boyer, P. D., Ed.; Academic Press: New York, 1971; Vol. III, p 1. (b) Lipscomb, W. N. *Proc. Natl. Acad. Sci. U.S.A.* **1973**, *70*, 3797. (c) Quiocho, F. A.; Lipscomb,

W. N. *Adv. Protein Chem.* **1971**, *25*, 1. (d) Lipscomb, *Chem. Soc. Rev.* **1972**, *1*, 319. (e) Breslow, R.; Wernick, D. L. *Proc. Natl. Acad. Sci. U.S.A.* **1977**, *74*, 1303. (f) Hayes, P. M.; Kollman, P. A. *J. Am. Chem. Soc.* **1976**, *98*, 3335.

(4) (a) Lindskog, S.; Henderson, L. E.; Kannan, K. K.; Liljas, A.; Hyman, P. O.; Strandberg, B. *The Enzymes*; Boyer, P. D., Ed.; Academic Press: New York, 1971; Vol. V, p 587. (b) Kannan, K. K., Notstrand, K.; Fridborg, S.; Lövgren, S.; Ohlsson, A.; Petef, M. *Proc. Natl. Acad. Sci. U.S.A.* **1975**, *72*, 51. (c) Resando, J. M. *Biochemistry* **1975**, *14*, 675. (d) Gupta, R. K.; Resando, J. M. *J. Biol. Chem.* **1975**, *250*, 2630. (e) Harrowfield, J. M.; Norris, V.; Sargeson, A. M. *J. Am. Chem. Soc.* **1976**, *98*, 7282.

(5) (a) Bränden, C.-I.; Jörnvall, H.; Eklund, H.; Furugren, B. *The Enzymes*, 3rd ed.; Boyer, P. D., Ed.; Academic Press: New York, 1975; Vol. XI, p 104. (b) Prince, R. H.; Huges, M. *Chem. Ind. (London)* **1975**, 648. (c) Zeppezauer, E.; Jörnvall, H.; Ohlsson, I. *Eur. J. Biochem.* **1975**, *58*, 95. (d) Dunn, M. F.; Biellmann, J.-F.; Branzant, G. *Biochemistry* **1975**, *14*, 1998. (e) Klingman, J. P.; Welsh, K. *Biochem. Biophys. Res. Commun.* **1976**, *70*, 878.

(6) Richardson, J. S.; Thomas, K. A.; Rubin, B. H.; Richardson, D. C. *Proc. Natl. Acad. Sci. U.S.A.* **1975**, *72*, 1349. (b) Rotilio, G.; Calabrese, L.; Mondovi, B.; Blumberg, W. E. *J. Biol. Chem.* **1974**, *249*, 3157. (c) Fee, J. A. *Biochim. Biophys. Acta* **1973**, *295*, 107. (d) Fridovich, I. *Annu. Rev. Biochem.* **1975**, *44*, 147. (e) Lippard, S. J.; Burger, A. R.; Ugurbil, K.; Pantoliano, M. W.; Valentine, J. S. *Biochemistry* **1977**, *16*, 1137. (f) Fridovich, I. *Acc. Chem. Res.* **1972**, *5*, 321. (g) Malmstrom, B. G.; Andreasson, L.-E.; Einhammar, B. R. *The Enzymes*; Boyer, P. D., Ed.; Academic Press: New York, 1975; Vol. XII, p 507.

(7) (a) Summers, M. F.; Toscano, P. J.; Bresciani-Pahor, N.; Nardin, G.; Randaccio, L.; Marzilli, L. G. *J. Am. Chem. Soc.* **1983**, *105*, 6259. (b) Bresciani-Pahor, N.; Geremia, S.; López, C.; Randaccio, L.; Zangrando, E. *Inorg. Chem.* **1990**, *29*, 1043. (c) Hansen, L. M.; Kumar, P. N. V. P.; Marynick, D. S. *Inorg. Chem.* **1994**, *33*, 728.

(8) (a) Retey, J. *Vitamin B_{12} and B_{12}-Proteins*; Kraeutler, B.; Arigoni, D.; Golding, B. T., Eds.; Wiley: Weinheim, 1998. (b) *B_{12}*; Dolphin, D., Ed.; Wiley-Interscience: New York, 1982.

(9) (a) Hay, B. P.; Finke, R. G. *J. Am. Chem. Soc.* **1986**, *108*, 4820. (b) Toraya, T.; Matsumoto, T.; Ichikawa, M.; Itoh, T.; Sugawara, T.; Mizuno, Y. *J. Biol. Chem.* **1986**, *261*, 9289. (c) Toraya, T.; Ishida, A. *Biochemistry* **1988**, *27*, 7677. (d) Pett, V. B.; Liebman, M. N.; Murray-Rust, P.; Prasad, K.; Glusker, J. P. *J. Am. Chem. Soc.* **1987**, *109*, 3207. (e) Sirovatka, J. M.; Finke, R. G. *Inorg. Chem.* **1999**, *38*, 1697.

(10) (a) Christianson, D. W.; Lipscomb, W. N. *J. Am. Chem. Soc.* **1985**, *107*, 2682. (b) Mealli, C.; Sabat, M.; Marzilli, L. G. *J. Am. Chem. Soc.* **1987**, *109*, 1593. (c) Zhu, L.; Kostic, N. M. *Inorg. Chem.* **1987**, *26*, 4194. (d) Hansen, L. M.; Kumar, P. N. V. P.; Marynick, D. S. *Inorg. Chem.* **1994**, *33*, 728. (e) Hansen, L. M.; Derecskei-Kovacs, A.; Marynick, D. S. *J. Mol. Struct.* **1998**, *431*, 53.

(11) (a) Brown, K. L.; Cheng, S.; Zou, X.; Li, J.; Chen, G.; Valente, E. J.; Zubkowski, J. D.; Marques, H. M. *Biochemistry* **1998**, *37*, 9704. (b) Garr, C. D.; Sirovatka, J. M.; Finke, R. G.; *J. Am. Chem. Soc.* **1996**, *118*, 11142.

(12) Lehn, J. M.; Kintzinger, J. P. *Nitrogen NMR*; Witanowski, M., Webb, G. A., Eds.; Plenum: London, 1973; pp 79−161.

(13) (a) Guibé, L. *Adv. Nucl. Quadrupole Reson.* **1974**, *1*, 375. (b) Marino, R. A. *Adv. Nucl. Quadrupole Reson.* **1974**, *1*, 391. (c) Oja, T. *Adv. Nucl. Quadrupole Reson.* **1974**, *1*, 401.

(14) Ke, S.-C.; Torrent, M.; Musaev, D. G.; Morokuma, K.; Warncke, K. *Biochemistry* **1999**, *38*. In press.

(15) Ashby, C. I. H.; Paton, W. F.; Brown, T. L. *J. Am. Chem. Soc.* **1980**, *102*, 2990.

(16) (a) Hemmingsen, L.; Ryde, U. *J. Phys. Chem.* **1996**, *100*, 4803. (b) Ha, T. K.; Keller, M. J.; Gunde, R.; Gunthard, H. H. *J. Mol. Struct.* **1996**, *364*, 161.

(17) (a) Redshaw, M.; Palmer, M. H.; Findlay, R. H. *Z. Naturforsch. A* **1979**, *34*, 220. (b) Palmer, M. H.; Simpson, I.; Findlay, R. H. *Z. Naturforsch. A* **1981**, *36*, 34.

(18) (a) Palmer, M. H.; Haq, M. M. I.; Stephenson, D.; Smith, J. A. S. *Chem. Phys. Lett.* **1986**, *127*, 615. (b) Palmer, M. H.; Gould, R. O.; Blake, A. J.; Smith, J. A. S.; Stephenson, D.; Ames, D. E. *Chem. Phys.* **1987**, *112*, 213. (c) Palmer, M. H.; Stephenson, D.; Smith, J. A. S. *Chem. Phys.* **1985**, *97*, 103.

(19) Eriksson, L. A.; Malkina, O. L.; Malkin, V. G.; Salahub, D. R. *Int. J. Quantum Chem.* **1997**, *63*, 575.

(20) (a) Kern, C. W.; Karplus, M. *J. Chem. Phys.* **1965**, *42*, 1062. (b) Prasad, G.; Keshari, V.; Chandra, P. *J. Mol. Struct.* **1989**, *192*, 253.

(21) Lucken, E. A. C. *Nuclear Quadrupole Coupling Constants*; Academic: New York, 1969.

(22) (a) Prasad, G.; Lal, A.; Chandra, P. *Theor. Chim. Acta* **1989**, *75*, 475. (b) Palmer, M. H. *Chem. Phys.* **1988**, *127*, 335. (c) Pati, R.; Srinivas, S.; Briere, T.; Das, T. P. *J. Phys. Chem.* **1995**, *99*, 9051.

(23) (a) Cummins, P. L.; Bacskay, G. B.; Hush, N. S.; Ahlrichs, R. *J. Chem. Phys.* **1987**, *86*, 6908. (b) Brown, R. D.; Head-Gordon, M. P. *Mol. Phys.* **1987**, *61*, 1183.

(24) (a) Ha, T. K.; Gunthard, H. H. *J. Mol. Struct.* **1993**, *300*, 619. (b) Schirmacher, A.; Winter, H. *Phys. Rev. A* **1993**, *47*, 4891. (c) Sundholm, D.; Pyykkö, P.; Laaksonen, L.; Sadlej, A. *Chem. Phys.* **1986**, *101*, 219. (d) Ha, T. K. *Z. Naturforsch. A* **1986**, *41*, 163. (e) Cernusak, I.; Diercksen, G. H. F.; Sadlej, A. J. *Chem. Phys.* **1986**, *108*, 45. (f) Winter, H.; Andrä, H. J. *Phys. Rev. A* **1980**, *21*, 581. (g) Olsen, J.; Sundholm, D. *Chem. Phys. Lett.* **1994**, *226*, 17.

(25) Tokman, M.; Sundholm, D.; Pyykkö, P.; Olsen, J. *Chem. Phys. Lett.* **1997**, *265*, 60.

(26) Kukolich, S. G.; Wofsy, S. C. *J. Chem. Phys.* **1970**, *52*, 5477.

(27) Cremer, D.; Krüger, M. *J. Phys. Chem.* **1992**, *96*, 3239.

(28) Griffiths, J. H.; Wardley, A.; Williams, V. E.; Owen, N. L.; Sheridan, J. *Nature* **1967**, *216*, 1301.

(29) O'Konski, C. T.; Ha, T.-K. *J. Chem. Phys.* **1968**, *49*, 5354.

(30) Åstrand, P.-O.; Ruud, K.; Mikkelsen, K. V.; Helgaker, T. *Mol. Phys.* **1997**, *92*, 89.

(31) (a) Hall, G. G.; Smith, C. M. *Int. J. Quantum Chem.* **1984**, *25*, 881. (b) Smith, C. M.; Hall, G. G. *Theor. Chim. Acta* **1986**, *69*, 63.

(32) (a) Besler, B. H.; Merz, K. M., Jr.; Kollman, P. A. *J. Comput. Chem.* **1990**, *11*, 431. (b) Singh, U. C.; Kollman, P. A. *J. Comput. Chem.* **1984**, *5*, 129.

(33) (a) Miertus, S.; Scrocco, E.; Tomasi, J. *Chem. Phys.* **1981**, *55*, 117. (b) Miertus, S.; Tomasi, J. *Chem. Phys.* **1982**, *65*, 239. (c) Cossi, M.; Barone, R.; Cammi, R.; Tomasi, J. *Chem. Phys. Lett.* **1996**, *255*, 327.

(34) Frisch, M. J.; Trucks, G. W.; Schlegel, H. B.; Scuseria, G. E.; Robb, M. A.; Cheeseman, J. R.; Zakrzewski, V. G.; Montgomery, J. A., Jr.; Stratmann, R. E.; Burant, J. C.; Dapprich, S.; Millam, J. M.; Daniels, A. D.; Kudin, K. N.; Strain, M. C.; Farkas, O.; Tomasi, J.; Barone, V.; Cossi, M.; Cammi, R.; Mennucci, B.; Pomelli, C.; Adamo, C.; Clifford, S.; Ochterski, J.; Petersson, G. A.; Ayala, P. Y.; Cui, Q.; Morokuma, K.; Malick, D. K.; Rabuck, A. D.; Raghavachari, K.; Foresman, J. B.; Cioslowski, J.; Ortiz, J. V.; Stefanov, B. B.; Liu, G.; Liashenko, A.; Piskorz, P.; Komaromi, I.; Gomperts, R.; Martin, R. L.; Fox, D. J.; Keith, T.; Al-Laham, M. A.; Peng, C. Y.; Nanayakkara, A.; Gonzalez, C.; Challacombe, M.; Gill, P. M. W.; Johnson, B.; Chen, W.; Wong, M. W.; Andres, J. L.; Gonzalez, C.; Head-Gordon, M.; Replogle, E. S.; Pople, J. A. *Gaussian 98*, Revision A.1; Gaussian, Inc.: Pittsburgh, PA, 1998.

(35) Åstrand, P.-O.; Ruud, K.; Mikkelsen, K. V.; Helgaker, T. *Mol. Phys.* **1997**, *92*, 89.Blackman, G. L.; Brown, R. D.; Burden, F. R.; Elsum, I. R. *J. Mol. Spectrosc.* **1976**, *60*, 63.

(36) (a) Lucken, E. A. C. *Nuclear Quadrupole Coupling Constants*; Academic: New York, 1969. (b) Smith, J. A. S. *Chem. Soc. Rev.* **1986**, *15*, 225.

(37) Palmer, M. H. *Z. Naturforsch. A* **1985**, *41*, 147.

(38) Murgich, J.; Aray, Y.; Soscun, H. J.; Marino, R. A. *J. Phys. Chem.* **1992**, *96*, 9198.

(39) Huber, S.; Ha, T.-K.; Bauder, A. *J. Mol. Struct.* **1997**, *413*−*414*, 93.

(40) Yamanouchi, K.; Kato, S.; Morokuma, K.; Sugie, M.; Takeo, H.; Matsumura, C.; Kuchitsu, K. *J. Phys. Chem.* **1987**, *91*, 828.

(41) Edmonds, D. T. *Phys. Rep.* **1977**, *29*, 233.

(42) García, M. L. S.; Smith, J. A. S.; Bavin, P. M. G.; Ganellin, C. R. *J. Chem. Soc., Perkin Trans. 2* **1983**, 1391.

(43) Omel'Chenko, Y. A.; Kondrasher, Y. D. *Sov. Phys. Crystallogr.* **1971**, *16*, 88.

(44) McMullan, R. K.; Epstein, J.; Ruble, J. R.; Craven, B. M. *Acta Crystallogr. B* **1979**, *35*, 688.

(45) Cummins, P. L.; Bacskay, G. B.; Hush, N. S. *Mol. Phys.* **1987**, *62*, 193.

(46) Cobb, J.; Haq, M. M. I.; Kurshid, M. M. P.; Smith, J. A. S.; Palmer, M. H. *Chem. Phys.* **1993**, *169*, 65.

(47) *CRC Handbook of Chemistry and Physics* 77th ed. (1996−1997); Lide, D. R., Ed.; CRC Press: New York, 1996.

(48) Savage, H. F. J.; Lindley, P. F.; Finney, J. L.; Timmins, P. A. *Acta Crystallogr. B* **1987**, *43*, 280.

(49) (a) Savage, H. F. J. *Biophys. J.* **1986**, *50*, 947. (b) Savage, H. F. J. *Biophys. J.* **1986**, *50*, 967.